CHIN. PHYS. LETT. Vol. 35, No. 7 (2018) 070502

Reconstruction of Intrinsic Thermal Parameters of Methane Hydrate and Thermal Contact Resistance by Freestanding 3ω Method *

Jia Li(李佳), Zhao-Liang Wang(王照亮)**, Gui-Ce Yao(姚贵策)

Energy and Power Department, China University of Petroleum (East China), Qingdao 266580

(Received 9 April 2018)

It is essential to obtain thermophysical properties of methane hydrate precisely with a freestanding probe for modeling and predicting thermal transport in gas hydrates. A method with a freestanding 3ω probe is presented to reconstruct the intrinsic thermal conductivity, thermal diffusivity, and thermal contact resistance of methane hydrate. Isolated from the thermal contact resistance, the intrinsic thermal conductivity of methane hydrate decreases between 250 K and 280 K and is 41% larger than the effective value at 253 K. More importantly, when the thermal contact resistance is isolated, the temperature dependence of intrinsic thermal conductivity shows a converse trend with the generally accepted glass-like feature at high temperature. Otherwise, thermal contact resistances measured in the experiment between the freestanding 3ω probe and the methane hydrate sample are extraordinary large. The freestanding 3ω method in this work is expected to measure the thermal property of methane hydrate more accurately.

PACS: 05.70.−a, 05.70.Np, 68.60.−p, 68.65.Ac DOI: 10.1088/0256-307X/35/7/070502

Methane hydrate is a typical clathrate hydrate which contains water cages and small guest molecules,[1] and mainly exists at the bottom of the seafloor and in permafrost regions.[2,3] Recently methane hydrate was extensively studied due to its unique thermal physical properties.[4−9] Various methods were applied to measure the thermal conductivity of methane hydrate, such as needle probe or hot-wire method,[6,9−12] hot plate cell method[13] and TPS method.[14−16] Ross and Anderson discovered the anomalous glass-like thermal conductivity behavior,[4] and the resonant scattering model was used to explain this phenomenon.[8,17−22] On the other hand, Krivchikov *et al.* found a different crystal-like thermal conductivity behavior under 90 K.[11,12] The MD simulation results of English *et al.* also proved this phenomenon.[16,23,24] However, most of these measured results are effective thermal conductivities, which include thermal contact resistance (TCR) due to the unavoidable imperfect contact. It is desirable to isolate the TCR from the effective thermal conductivity. Yet the 3ω method is thought to be a good way to measure the intrinsic thermal conductivity since it can separate the TCR by changing the test frequency. Although the 3ω method was widely used to test the thermal properties of materials,[25,26] it was rarely used to measure the hydrate since it is hard to deposit the metal probe directly on porous hydrate. In addition to this, thermal diffusivity of methane hydrate was rarely studied in the measurements.[27,28] In this Letter, firstly an experimental system including gas hydrate formation and freestanding 3ω apparatus is established. Secondly, the 3ω method modified for freestanding film is established to thermally characterize the thermal conductivity and thermal diffusivity of the Kapton film, and then TCR at the probe-hydrate interface, thermal conductivity and thermal diffusivity are simultaneously reconstructed. Finally, the temperature dependence of thermal properties is analyzed.

In the experiment, the first step is to generate methane hydrate. Figure 1 shows the methane hydrate formation system. The procedure is as follows: firstly, the vacuum pump is used to remove impurity gas in the reactor and pipelines. Then water and methane gas are sequentially added to the reactor. To ensure that the probe can be in contact with methane hydrate, the water level should be 5 mm higher than the freestanding sensor according to the experimental requirements. Next open the data collector to record the temperature and pressure signals in the reactor. For the reactor, the temperature is controlled by a cryogenic thermostat through external circulation of ethanol refrigerating liquid in the cooling jacket. When the temperature remains constant, it comes into the induction period for methane hydrate formation. The hydrate formation comes to an end until the pressure signal no longer changes. To measure the thermal properties of the hydrate, a freestanding 3ω probe is designed as shown in Fig. 2. The freestanding 3ω probe with length of 11 mm and width of 100 μm is welded at four pads. The accurate length and width of the freestanding 3ω probe are determined from calibration using distilled water and air as the standard samples. The sensor element in the probe is made of nickel since it is more sensitive to temperature rise than platinum. Meanwhile, a Kapton film with thickness of 25 μm is encapsulated on both sides of the four pads structure. The temperature fluctuation of the 3ω probe is controlled within

*Supported by the National Natural Science Foundation of China under Grant No U1262112, and the Fundamental Research Funds for the Central Universities under Grant No 18CX06035A.

**Corresponding author. Email: wzhaoliang@126.com

© 2018 Chinese Physical Society and IOP Publishing Ltd

± 1 K by changing the test voltage and frequency.

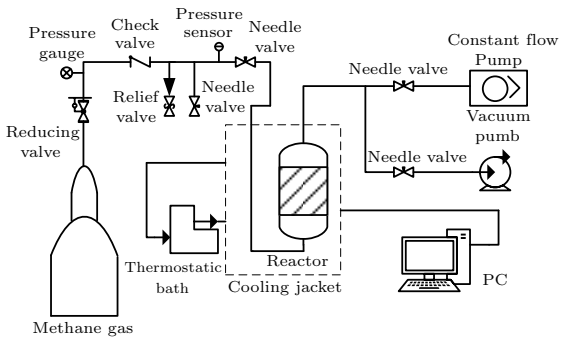

Fig. 1. Methane hydrate formation system.

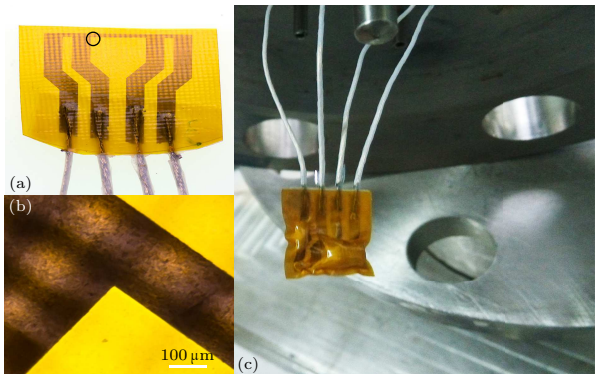

Fig. 2. Free-standing 3ω probe and reactor cell.

In the 3ω method system, the signal generator sends out an ac voltage signal at a frequency of ω, which converts into a current signal at the same frequency after the first operational amplifier. The current signal then acts on the potentiometer and metal bridge of the freestanding probe and generates voltage signals, which become differential signals after the second and third operational amplifiers. Passing through preoperational amplifier they are sent to a lock-in amplifier and then the 3ω signal is retrieved.

The temperature fluctuation of the freestanding film can be described as[29]

$$\bar{\theta}_{2\omega} = \sum_{n=1}^{\infty}\sum_{m=1}^{\infty} \frac{-\xi_{m,n}}{2\sqrt{\gamma_{m,n}^2 + 4\omega^2}} \cdot \frac{\sin((m+1/2)\pi)(1-\cos(n\pi))}{n\pi}, \quad (1)$$

where $\bar{\theta}_{2\omega}$ is the temperature fluctuation at 2ω, ω is the angular frequency, k, α and d are the thermal conductivity, the thermal diffusivity and the half thickness of the Kapton film, P represents the heating power, b and l are the half width and the length of the freestanding metal heater, $\xi_{m,n}$ and $\gamma_{m,n}$ are coefficients associated with k, α, P, d, l and b.

In the measurement, the whole sample can be treated as a two-layer structure. The surface thermal impedance for the two-layer system is introduced as

$$Z = \frac{\bar{\theta}_{2\omega}}{P/bl} = \frac{2}{\pi}\int_0^{\infty} \frac{\sin^2\beta}{\beta^2} z(\beta)_2 d\beta. \quad (2)$$

Taking TCR into account, the corrected thermal impedance becomes

$$\bar{z}(\beta)_1 = z(\beta)_1 - TCR. \quad (3)$$

It is a typical multi parameter fitting problem to calculate the unknown factor with third harmonic data measured in experiment and Eqs. (1)–(3). The objective function is minimized by the iterative algorithm after bringing the initial value of each parameter into it, and the parameters that need to be fitted can be determined simultaneously.

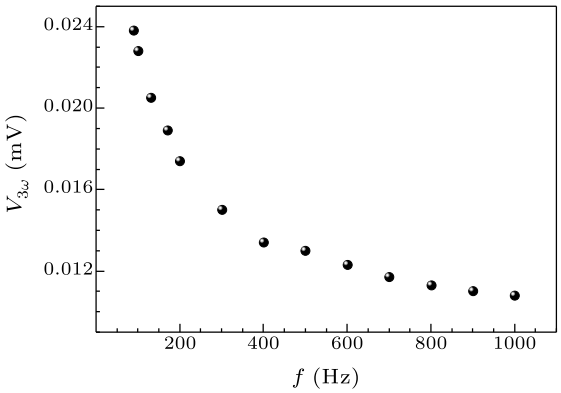

Fig. 3. Relationship between frequency and 3ω amplitude of voltage for the Kapton film.

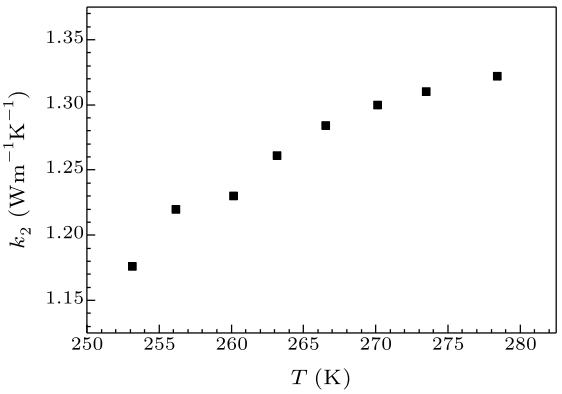

Fig. 4. Relationship between thermal conductivity and temperature for the Kapton film.

Figure 3 shows the relationship between frequency and 3ω amplitude of voltage for the Kapton film. As we can see, the third harmonic oscillation amplitude decreases rapidly at frequency 10–1000 Hz. The thermal conductivity of the Kapton film is shown in Fig. 4. Using a temperature-controlled thermostatic bath, the measurements are repeated over 250–280 K. Afterwards, the least square method is used to fit the measurement data. Different from the strong temperature dependence shown in Fig. 4, the thermal diffusivity of the Kapton film is about 0.77×10^{-7} m^2/s

and shows very weak temperature dependence over the temperature range.

The relationship between frequency and 3ω amplitude of voltage for the methane hydrate sample at 253 K is plotted in Fig. 5. At rather low frequency (< 10 Hz), the thermal penetration length far exceeds the thickness of the Kapton film and the linear part of the curve is more sensitive to the thermal properties of methane hydrate. TCR at the interface between the Kapton film and methane hydrate, thermal conductivity and diffusivity of methane hydrate are simultaneously determined by fitting the third harmonic voltage shown in Fig. 5.

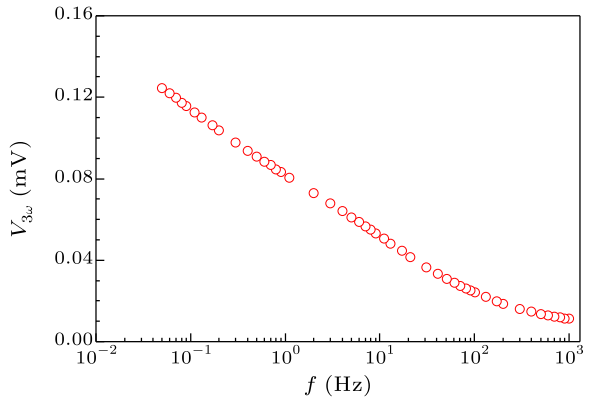

Fig. 5. Relationship between frequency and 3ω amplitude of voltage for methane hydrate.

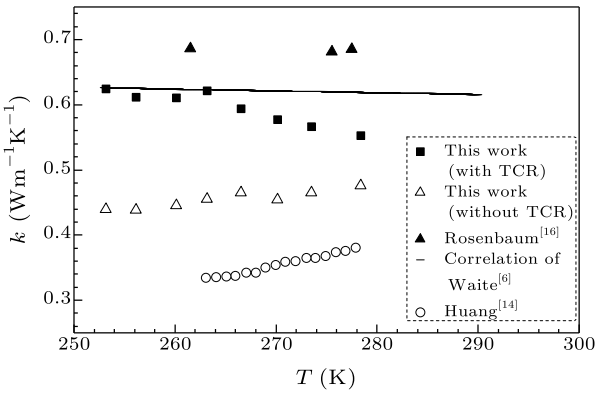

Fig. 6. Temperature dependence of thermal conductivity for methane hydrate.

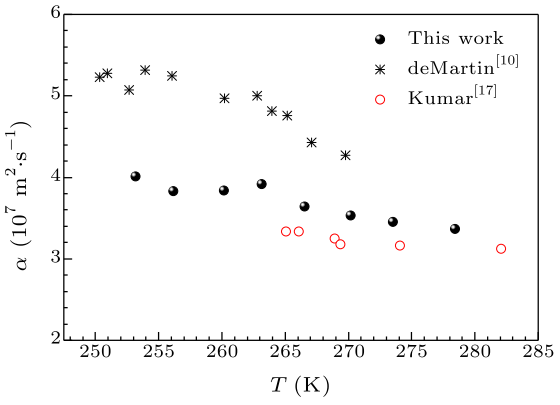

Fig. 7. Temperature dependence of thermal diffusivity for methane hydrate.

The temperature dependence of thermal conductivity for methane hydrate is shown in Fig. 6. It can be seen that the effective thermal conductivity, if TCR is included, becomes smaller and the temperature dependence shows a trend which is consistent with the generally glass-like results by TPS. Isolated from TCR, the intrinsic thermal conductivity of methane hydrate decreases between 250 K and 280 K and is 41% larger than the effective value at 253 K, while the intrinsic thermal conductivity using the freestanding 3ω method is much larger than those by TPS on uncompacted methane hydrate[14] and close to the values predicted by Waite *et al.*[6] from 250 to 280 K. The difference in thermal conductivity by different methods is mainly caused by two factors. One is the interfacial effect, e.g., roughness near the interface between the probe and the hydrate, the properties of the interfaces between the phases within the hydrate. The other is the influence of different concentrations of impurities, porosity and different sample preparation processes on thermal properties.

The systematic decrease of thermal diffusivity for methane hydrate is represented in Fig. 7 at different temperatures. For further comparison, the thermal diffusivities of methane hydrate at different temperatures calculated by deMartin[10] and Kumar *et al.*[27] are also shown in Fig. 7. The data by the freestanding 3ω method in this work and of Kumar *et al.*[27] are close and have the same magnitude as data of deMartin.[10] This seems to indicate that porosity may have less effect on thermal diffusivity than thermal conductivity which has been discussed by Waite *et al.*[6] and Rosenbaum *et al.*[16]

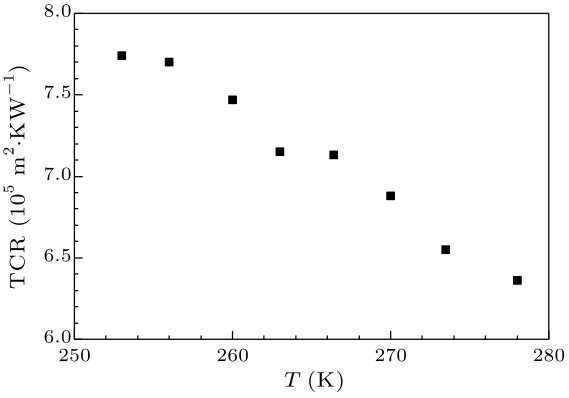

Fig. 8. Temperature dependence of TCR.

Our data for the temperature dependence of the overall TCR for the interface between freestanding probe and methane hydrate is shown in Fig. 8. We observe a significant temperature dependence of TCR. The temperature dependence yields information about the freestanding probe-methane hydrate phonon interface transmittance. Since an elastic two-phonon process produces a TCR that is approximately independent of temperature at high temperature, it can be expected that multiple-phonon inelastic scattering events including three or four-phonon processes of the

type are excited and will contribute a new channel to the thermal conductance that increases with temperature. Moreover, for the interface between the freestanding probe and methane hydrate, the contacting condition may be another factor resulting in the temperature dependence trend. Temperature-induced interfacial diffusion or rearrangement may lead to closer contact between freestanding probes and methane hydrate and somewhat intensify heat transfer.

The uncertainties of the measured thermal parameters can be expressed as $\frac{\delta X}{X} = \sqrt{(\frac{\partial V_{3\omega}}{\partial X})^2(\frac{\delta V_{3\omega}}{V_{3\omega}})^2}$, where X represents the fitted thermal parameter. In the measurement, the uncertainties in the intrinsic thermal conductivity, intrinsic thermal diffusivity and thermal contact resistance measurements are around 4.0–6.5%, 5.5–7.0% and 14.5–18.5%, respectively. The maximum temperature rise of the heater is limited to around 0.2 K.

In summary, a method with a freestanding 3ω probe has been presented to reconstruct the thermal conductivity, thermal diffusivity of methane hydrate, and thermal contact resistance. Compared with other methods, this method has advantages in measuring TCR at the interface of a freestanding probe and the hydrate sample. The measured value of the thermal conductivity for methane hydrate is significantly larger than the other values by TPS, which enhances the demand for direct freestanding probe measurements rather than using effective values including TCR when measuring thermal properties of methane hydrate. The important role played by the temperature dependence trend of the measured TCR cannot be ignored in the generally glass-like feature of methane hydrate. The thermophysical measurements on methane hydrate described in this work are likely to throw new light on thermal transport.

References

[1] Sloan E D 1998 *Clathrate Hydrates of Natural Gases* II (New York: Marcel Dekker Inc)
[2] Kerr R A 2004 *Science* **303** 946
[3] Buffett B A 2000 *Annu. ReV. Earth Planet. Sci.* **28** 477
[4] Ross R G, Andersson P and Bäckström G 1981 *Nature* **290** 322
[5] English N J and Tse J S 2010 *Energies* **3** 1934
[6] Waite W F, Stern L A, Kirby S H, Winters W J and Mason D H 2007 *Geophys. J. Int.* **169** 767
[7] Tse J S and White M A 1988 *J. Phys. Chem.* **92** 5006
[8] Tse J S 1994 *J. Inclusion Phenom. M0l. Recognit. Chem.* **17** 259
[9] Gupta A, Kneafsey T J, Moridis G J, Seol Y, Kowalsky M B and Sloan E D 2006 *J. Phys. Chem.* B **110** 16384
[10] Demartin B J 1953 *J. Soc. Psychol.* **38** 99
[11] Krivchikov A I, Gorodilov B Y, Korolyuk O A, Manzhelii V G, Conrad H and Press W 2005 *J. Low Temp. Phys.* **139** 693
[12] Krivchikov A I, Gorodilov B Y, Korolyuk O A, Manzhelii V G, Romantsova O O, Conrad H, Press W, Tse J S and Klug D D 2006 *Phys. Rev.* B **73** 064203
[13] Cook J G and Leaist D G 1983 *Geophys. Res. Lett.* **10** 397
[14] Huang D Z and Fan S S 2004 *J. Chem. Eng. Data* **49** 1479
[15] Huang D Z, Fan S S, Liang D Q and Feng Z P 2005 *Chin. J. Geophys.* **48** 1201
[16] Rosenbaum E J, English N J, Johnson J K, Shaw D W and Warzinski R P 2007 *J. Phys. Chem.* B **111** 13194
[17] Inoue R, Tanaka H and Nakanishi K 1996 *J. Chem. Phys.* **104** 9569
[18] Tse J S, Shpakov V P, Murashov V V and Belosludov V R 1997 *J. Chem. Phys.* **107** 9271
[19] Tse J S, Ratcliffe C I, Powell B M, Sears V P and Handa H P 1997 *J. Phys. Chem.* **101** 4491
[20] Tse J S, Shpakov V P, Belosludov V R, Trouw F and Handa Y P 2001 *Europhys. Lett.* **54** 354
[21] Baumert J, Gutt C, Shpakov V P, Tse J S, Krisch M, Müller M, Requardt H, Klug D D, Janssen S and Press W 2003 *Phys. Rev.* B **68** 174301
[22] Tse J S, Klug D D, Zhao J Y, Sturhahn W, Alp E E, Baumert J, Gutt C, Johnson M R and Press W 2005 *Nat. Mater.* **4** 917
[23] Krivchikov A I, Korolyuk O A and Romantsova O O 2007 *Low Temp. Phys.* **33** 612
[24] English N J 2008 *Mol. Phys.* **106** 1887
[25] Cahill D G 1990 *Rev. Sci. Instrum.* **61** 802
[26] Cahill D G, Katiyar M and Abelson J R 1994 *Phys. Rev.* B **50** 6077
[27] Kumar P, Turner D and Sloan E D 2004 *J. Geophys. Res.* **109** 01207
[28] Turner D J, Kumar P and Sloan E D 2005 *Int. J. Thermophys.* **26** 1681
[29] Jain A and Goodson K E 2008 *J. Heat Transfer* **130** 102402